Cell Chemical Biology

Review

Current advances in photocatalytic proximity labeling

Steve D. Knutson,[1,2] Benito F. Buksh,[1,2] Sean W. Huth,[1,2] Danielle C. Morgan,[1,2] and David W.C. MacMillan[1,2,*]
[1]Merck Center for Catalysis at Princeton University, Princeton, NJ 08544, USA
[2]Department of Chemistry, Princeton University, Princeton, NJ 08544, USA
*Correspondence: dmacmill@princeton.edu
https://doi.org/10.1016/j.chembiol.2024.03.012

SUMMARY

Understanding the intricate network of biomolecular interactions that govern cellular processes is a fundamental pursuit in biology. Over the past decade, photocatalytic proximity labeling has emerged as one of the most powerful and versatile techniques for studying these interactions as well as uncovering subcellular trafficking patterns, drug mechanisms of action, and basic cellular physiology. In this article, we review the basic principles, methodologies, and applications of photocatalytic proximity labeling as well as examine its modern development into currently available platforms. We also discuss recent key studies that have successfully leveraged these technologies and importantly highlight current challenges faced by the field. Together, this review seeks to underscore the potential of photocatalysis in proximity labeling for enhancing our understanding of cell biology while also providing perspective on technological advances needed for future discovery.

INTRODUCTION

Cellular function is orchestrated by a vast network of interactions between proteins, nucleic acids, and other biomolecules.[1–3] Cells maintain their internal environment through complex associations with ion channels and transporters to regulate intracellular solute concentrations,[4] pH,[5] and temperature.[6] In addition, DNA replication, transcription, and translation are coordinated by a series of dynamic biomolecular interactions, ensuring faithful transmission of genetic information.[7,8] Enzymes within the cell also catalyze specific biochemical reactions by binding to small molecule substrates,[9] while cell-surface receptors sense and transduce environmental signals by recognizing specific ligands.[10] Lastly, small-molecule drugs typically act by either inhibiting or enhancing specific biomolecular interactions, and targeting these associations allows for the development of therapies that can treat a wide range of diseases.[11]

Given the importance of these biomolecular interactions, key technical approaches have been developed over the years to map and understand these networks and gain insight into cellular mechanics. One of the first general methods developed for characterizing interactomes involved purifying a target protein or biomolecule of interest from a complex cell mixture.[12] Co-immunoprecipitation (co-IP), although established in the mid-20th century,[13] can still be powerfully applied today to identify interactors with modern sequencing and mass spectrometry workflows.[14] Confirmation of these interactions can then be assayed using the yeast two-hybrid (Y2H) system, whereby reconstitution of a transcription factor leads to reporter gene expression.[15] Although both systems revolutionized the identification and screening of protein interactions, these approaches require significant prior knowledge about targets of interest and are less suited to complex biological settings, especially in the case of membrane protein interactome discovery.

Proximity labeling has rapidly emerged to address these limitations and is one of the most robust techniques currently available to profile biomolecular interactions with high spatial and temporal precision.[16,17] From its initial technical development in the early 2000s, a multitude of platforms have now been established over the past two decades. Photocatalytic proximity labeling in particular has experienced significant effort and interest in recent years given the high level of spatial and temporal control that light activation enables. In this review, we will summarize the basic principles of proximity labeling for generating biological insight as well as provide historical perspectives and recent developments in photocatalytic proximity platforms. We will discuss the advent of different catalytic manifolds and explore their innate chemical mechanisms. In addition, we will compare their distinct methodological and technical advantages and highlight key recent studies implementing these platforms in different biological contexts. Lastly, we provide perspective on both the opportunities and challenges for the field in order to use these platforms to enhance our future understanding of cell and tissue physiology.

BASIC PRINCIPLES OF PROXIMITY LABELING AND PHOTOCATALYSIS

The concept of proximity labeling has its roots in the early 2000s when researchers sought to develop unbiased methods for mapping protein interactions in live cells. Traditional methods for analyzing biomolecular interactions (including co-IP and Y2H)

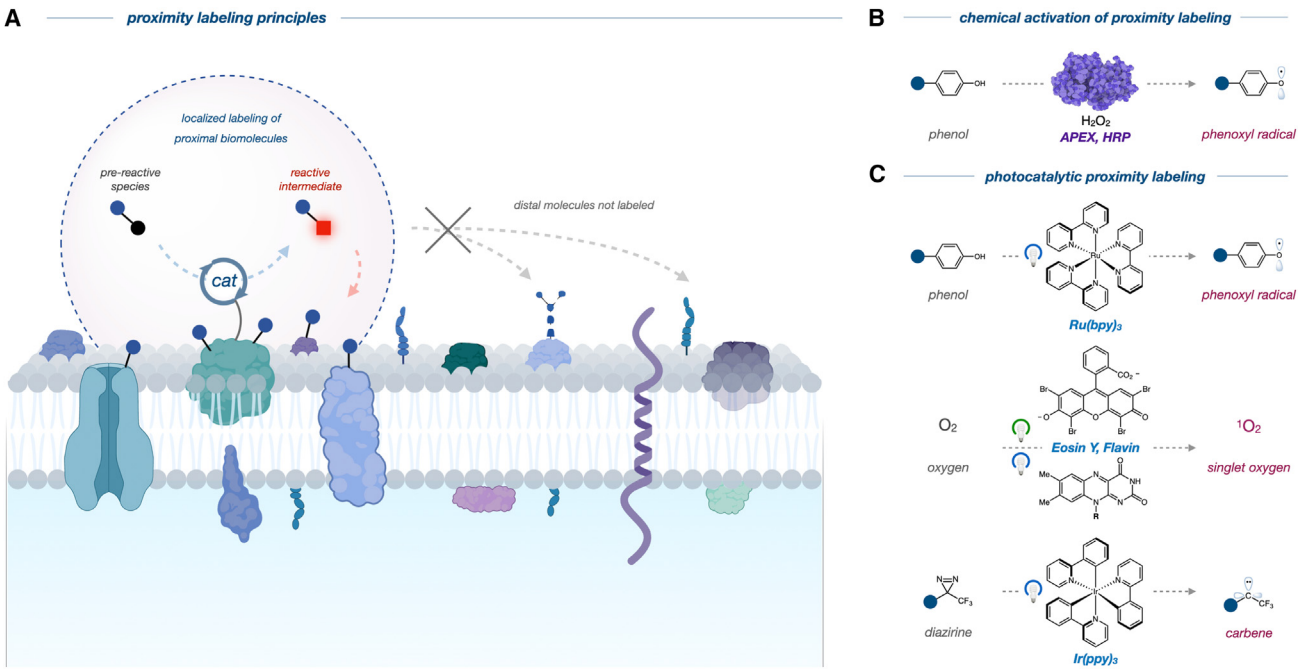

Figure 1. General principles and activation modes in proximity labeling

(A) A catalyst (cat) is localized to a biomolecule of interest to generate a reactive intermediate from an inert, pre-reactive species. This reactive probe has a limited range of diffusion such that only proximal biomolecules are covalently tagged for further isolation, identification, and characterization.

(B) Chemically triggered proximity labeling, as demonstrated by APEX/HRP peroxidase enzyme catalysts which utilize H_2O_2 to generate phenoxyl radicals from a phenol precursor.

(C) Selected examples of photocatalytic proximity labeling manifolds, which are activated by various visible light sources to generate reactive intermediates (radicals, singlet oxygen, carbenes, etc).

provide only a static snapshot of interactions and require specific antibodies for each target. To overcome these challenges, proximity labeling methods were thus designed to capture short-lived, transient interactions in an unbiased manner and provide spatial context to these associations. The underlying principle of this technique entails selective labeling of biomolecules that are in close proximity to a target of interest in the native cellular context (Figure 1A). A catalyst is first localized to a desired target, which then generates reactive intermediates to covalently modify nearby molecules with a label, such as biotin, enabling subsequent isolation and characterization. The first proximity labeling technique, termed "biotin identification (BioID)," leveraged a mutant *Escherichia coli* biotin ligase (BirA) to covalently label nearby proteins.[18,19] While this method was a breakthrough and established the framework for all subsequent proximity labeling platforms, it also displayed both low efficiency and spatiotemporal control over labeling. Building off this initial platform, the development of APEX (enhanced ascorbate peroxidase) and phenoxyl radical-based proximity labeling represented a significant technical advance and remains one of the most widely utilized labeling methods today.[20,21] APEX is activated with hydrogen peroxide to generate phenoxyl radicals from a biotin-phenol precursor to covalently label nearby proteins (Figure 1B). The addition of a chemical trigger (H_2O_2) provided greater control over labeling compared to ligase-tagging with BioID, allowing researchers to study interactions and subcellular structures with higher accuracy. Despite these advantages, chemical activation and quenching of enzyme catalysts is still governed by diffusion in biological systems, limiting the overall spatial and temporal resolution. These inherent challenges underlie the motivation for developing the photocatalytic proximity labeling platforms that are used today.

In parallel with APEX development, phenoxyl radicals were subsequently shown to be photochemically generated with ruthenium (Ru) photocatalysts (Figure 1C),[22,23] demonstrating some of the first photocatalytic activation modes for generating the requisite reactive intermediates. Similarly, research exploring photosensitizers, which can absorb and transfer light energy to other molecules, expanded the chemical capabilities of proximity labeling components for use in molecular biology. Catalytic photosensitizers can locally generate reactive species upon exposure to light, ultimately leading to covalent modification of proximal biomolecules. Xanthene- and flavin-based chromophores are both well-suited for this application, as they both undergo visible light activation to enter an excited singlet state (S_1) followed by triplet state (T_1) transition. If the triplet excited chromophore encounters molecular oxygen and is quenched through energy transfer, singlet oxygen is subsequently generated and induces oxidation in nearby biomolecules (Figure 1C).[24,25] This reactivity has been successfully leveraged for proximity profiling of subcellular RNA distributions with HaloTag-compatible bromofluorescein sensitizers (Halo-seq).[26,27] Additionally, the genetically encodable, flavin-binding protein miniSOG (miniature singlet-oxygen-generator) has been utilized for RNA, DNA, and protein interactome profiling.[28–31] Although peroxidase and singlet oxygen-based

platforms have shown great utility, these reactive intermediates are also relatively long-lived and not quenched by water, resulting in a more diffuse labeling radius that is dozens to hundreds of nanometers away from the catalyst.[32,33] However, depending on the intracellular context, these labeling radii may be reduced when confined to small subcellular compartments and organelles or if reactive intermediates are quenched with intracellular compounds containing thiols or other nucleophiles.

To improve spatial resolution, our group has recently developed a "microenvironment mapping" (μMap) photocatalytic proximity labeling platform.[34] In this system, iridium (Ir) photocatalysts, upon blue light irradiation, convert diazirines into highly reactive carbenes through a Dexter energy transfer (EnT) mechanism (Figure 1C). Carbenes are both short-lived ($T_{1/2}$ ~1 ns) and quenched by water, resulting in a high-resolution labeling radius (~2 nm).[32] Separate efforts have also established photocaged quinone methides as a distinct reactive probe, originally as a genetically encodable photocrosslinking reactive group. More recent studies have applied these in the photocatalytic decaging-enabled proximity labeling (CAT-Prox) platform for both intracellular organelle composition mapping and cell-surface microenvironment profiling.[35–38] This work has coincided with the development of several other light-activated photocatalytic proximity labeling platforms over the past 5 years (Table 1), reflecting the utility of these systems for elucidating novel biology and underscoring the versatile photochemistry underlying each system. In this review, we will specifically focus on photocatalytic systems and describe recent studies that harness these platforms to discover new biology. These platforms are distinct from that of traditional photoaffinity labeling (PAL), wherein photo-reactive amino acid analogs containing diazirine or benzophenol functional groups are incorporated into proteins facilitating interactor labeling upon UV irradiation.[39] PAL has been reviewed extensively elsewhere,[17,40] and this review will emphasize catalytic systems that generate free reactive species that diffuse and tag nearby interactors. In addition to describing existing photocatalytic proximity labeling platforms, we also discuss contemporary needs and novel technical developments in next-generation systems.

PROFILING CELL-SURFACE INTERACTOMES WITH PHOTOCATALYTIC PROXIMITY LABELING

Cell-surface proteins play pivotal roles in mediating intercellular communication, serving as both environmental sensors as well as adaptors for receiving, transducing, and trafficking biomaterials. Despite the importance of these networks, studying cell surface interactomes remains a significant challenge. Many cell surface proteins exhibit high turnover rates and are unstable once removed from the plasma membrane. The cell surface is also highly non-uniform and is composed of diverse microdomains and fluid regions. Proximity labeling has emerged as a powerful tool to address these challenges and unravel the intricacies of cell surface protein networks. By targeting specific cell surface receptors, proximity labeling allows the mapping of receptor-ligand interactions, which is often the first step toward elucidating signaling pathways and understanding how cells respond to external stimuli. Cell-surface-focused experiments in proximity labeling are straightforward to design using a photocatalyst and a targeting agent of choice (Figure 2A). In particular, utilizing an antibody against a protein of interest is one of the most common targeting methods, and almost any photocatalyst can be subsequently conjugated using any number of reactive groups on the antibody (amines, sulfhydryls, unnatural amino acid incorporation, sugar oxidation, etc.).[41] The first μMap experiments on living cells utilized Ir-conjugated antibodies targeting CD45, CD47, and CD29, revealing unique proteomic signatures specific to each protein's microenvironment.[34] We also explored the programmed-death ligand 1 (PD-L1) in human B cells, which plays a pivotal role as an immune checkpoint ligand in cancer and is the primary mechanism for the monoclonal antibody therapeutic KeyTruda (pembrolizumab).[42] PD-L1-targeted μMap revealed and validated CD30 and CD300A as new interactors, which may play key unknown roles in immune checkpoint pathway crosstalk. In addition, μMap was performed in a two-cell system composed of a T cell/antigen-presenting cell (APC) immunosynapse to enable μMap at the interface of two cells, demonstrating the initial concept of both *cis*-labeling at the microenvironment of interest but also *trans*-labeling of proteins from the interacting cell. Similar efforts by Oslund and colleagues using PhoTag (flavin catalyst) for synaptic labeling across the PD-1/PD-L1 axis were accomplished within a mixed population of PBMCs and Raji cells.[43] PhoTag also cleverly combined this platform with oligonucleotide-barcoded antibodies, facilitating a multiomics single-cell sequencing approach for concurrent measurement of biotinylation, protein, and mRNA levels within the same individual cell. Additionally, the Wollscheid group developed the LUX-MS platform, which employs a rhodamine-based singlet oxygen generator, was used to investigate the major histocompatibility complex (MHC): T cell receptor (TCR) immunosynapse.[44] Utilizing stable isotope labeling by amino acids in cell culture (SILAC) with mouse dendritic and T cells in combination with a catalyst-conjugated immunogenic peptide ligand gp33,[45] LUX-MS observed a light-dependent enrichment of key components of the TCR primary signaling axis, such as MHC class I, CD8, CD86, and the entire CD2-CD48 axis, which has been reported to govern cellular directionality.[46] Together, these studies highlight the power of antibody-directed photocatalytic proximity labeling to capture a comprehensive snapshot of the cell-surface proteome and rapidly identify interactions in immune synapse formation and cell signaling.

Photocatalytic proximity labeling can also be used to evaluate interactions between host cells and various pathogens through direct incorporation of photocatalysts into viral/bacterial components or even intact infectious particles (Figure 2A). For example, μMap has now been used in two parallel studies to understand viral pathogenesis in severe acute respiratory syndrome coronavirus 2 (SARS-CoV-2). While angiotensin-converting enzyme 2 (ACE2) serves as the primary entry receptor, its expression varies across tissues and implies the involvement of auxiliary factors. To identifying these interactions, our group conjugated Ir photocatalysts to the Wuhan spike protein and utilized μMap to profile interactions in Calu-3 human lung cells.[55] Our results revealed at least 8 novel candidate receptors, and we validated that co-expression of ACE2 with neuropilin-2 (NRP2), ephrin receptor A7 (EPHA7), solute carrier family 6 member 15 (SLC6A15), or myelin and lymphocyte protein 2 (MAL2) significantly enhanced viral uptake. In a parallel

Table 1. Recently developed photocatalytic proximity labeling platforms

Name/Acronym	Publication Year	Catalyst	Reactive intermediate (precursor)	Light wavelength	Half-life	Experimental notes
Chromophore-assisted proximity labeling and sequencing (CAP-seq)[29]	2019	miniSOG protein (flavin)	singlet oxygen (O_2)	blue (450 nm)	4 μs[33]	• Genetically encodable • Labeled RNA captured with propargylamine reagent
Microenvironment mapping (μMap)[34]	2020	Iridium complex	carbene (diazirine)	blue (450 nm)	1 ns	• Not genetically encodable
LUX-MS[44]	2021	Thiorhodamine	singlet oxygen (O_2)	green (~590 nm)	4 μs	• Not genetically encodable • Labeled proteins captured with biocytin hydrazide reagent
Photocatalytic decaging-enabled proximity labeling (CAT-Prox)[37]	2021	Iridium complex	quinone methide (photocaged)	blue (450 nm)	<1 s[47]	• Not genetically encodable • Mitochondrial targeting
Proximity Histidine Labeling by Umpolung Strategy[48]	2021	Ruthenium complex	singlet oxygen (O_2)	blue (450 nm)	4 μs	• Not genetically encodable • Labeled proteins captured with 1-methyl-4-arylurazole reagent
Halo-seq[26]	2022	dibromofluorescein	singlet oxygen (O_2)	green (~500 nm)	4 μs	• Not genetically encodable • Labeled RNA captured with propargylamine reagent
Photoactivation-dependent proximity labeling (PDPL)[30]	2022	miniSOG protein (flavin)	singlet oxygen (O_2)	blue (450 nm)	4 μs	• Genetically encodable • Labeled proteins captured with 3-ethynylaniline reagent
Photocatalytic cell tagging (PhoTag)[43,49]	2022	riboflavin tetraacetate (RFT)	phenoxyl radical (phenol)	blue (450 nm)	100 μs	• Not genetically encodable
μMap-Red[50]	2022	Tin complex	aminyl radical (d azide)	red (660 nm)	50 μs[51]	• Not genetically encodable
Targeted aryl azide activation via deep red-light[52]	2023	Osmium complex	nitrene (aryl azide)	red (660 nm)	200 μs[53]	• Not genetically encodable
Reactive oxygen species (ROS)-induced protein labeling and identification (RinID)[31]	2023	miniSOG protein (flavin)	singlet oxygen (O_2)	blue (450 nm)	4 μs	• Genetically encodable • Labeled proteins captured with biotin aniline or propargylamine
Light-induced Interactome Tagging (LITag)[54]	2023	LOV protein (flavin)	singlet oxygen (O_2)	blue (450 nm)	4 μs	• Genetically encodable • Labeled proteins captured with phenol or aniline reagent

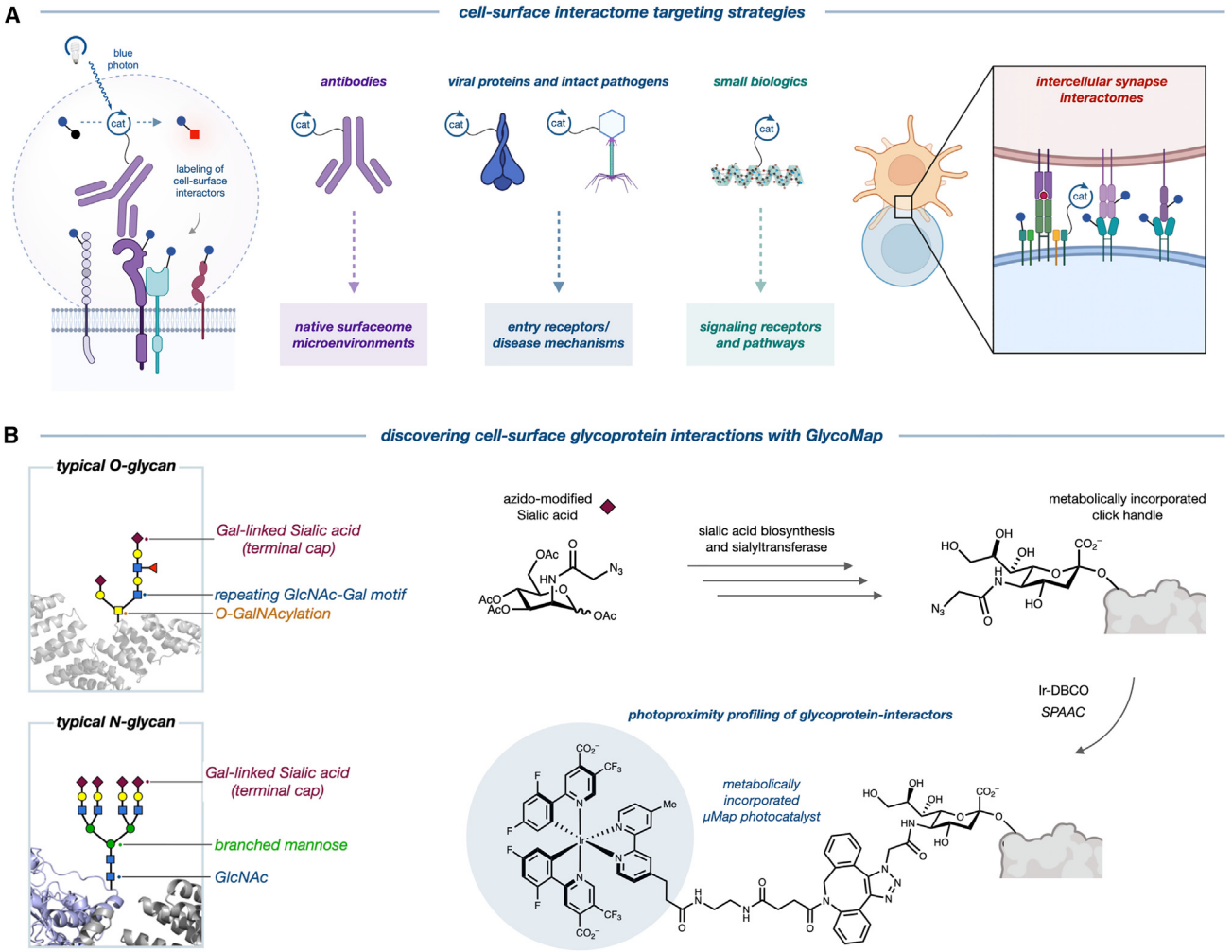

Figure 2. Biological insights generated from cell-surface interactome profiling with photocatalytic proximity labeling

(A) Cell-surface biomolecules can be probed with a variety of photocatalyst-conjugated targeting agents, including antibodies, recombinant viral proteins, intact pathogens/phages, and small biologics (cytokines, peptides, etc.). Additionally, appropriate catalyst localization can be used to profile synaptic interactions between two cells.

(B) Bioorthogonal click chemistry and metabolic incorporation of modified sugars into native glycoproteins enables photoproximity profiling of sialylation-dependent changes in protein microenvironments (GlycoMap).

study, Datta and coworkers utilized μMap to interrogate interactions between the SARS-CoV-2 spike protein and ACE2-expressing HEK293T cells.[56] This screen identified the co-receptor NRP1 and revealed several novel interactions with the spike subunit. Through knockdown and overexpression models, the team identified prostaglandin F2 receptor inhibitor (PTGFRN) and ephrin receptor beta 1 (EFNB1) as verified viral entry factors. In a related but distinct application of pathogen proximity labeling, the Wollscheid group utilized LUX-MS via an SOG catalyst-conjugated bacteriophage to identify cell wall entry components on Gram-positive *Listeria monocytogenes*, displaying enrichment of cell wall-associated internalins A and B that mediate cell invasion.[44] Together, these reports demonstrate the power of utilizing photocatalytic proximity labeling for studying host-pathogen interactions, and we predict that this particular application will continue across disciplines as new pathogens emerge.

Profiling surface glycoproteins is a major challenge in cell biology, yet these biomolecules play key roles in cell adhesion, signaling, and immune response.[57–59] Glycosylation can profoundly influence protein structure and stability, in turn altering both its function and interactome.[60] This area is of particular clinical interest as well, given that dysregulated glycosylation is implicated in both cancer and neurodegenerative disorders.[61] Proximity labeling provides several technical advantages for studying these interactomes, and our group developed an approach for mapping cell-surface glycoproteins, which we term GlycoMap (Figure 2B).[62] In particular, this approach focuses on sialic acid as a terminal sugar in glycated proteins. In many cancer types, overexpression of sialyltransferases and hypersialylation are hallmarks of oncogenesis,[63] promoting tumor progression through proposed pathways of immune evasion and metastatic spread.[64–66] However, the underlying mechanisms of these phenotypes remain elusive, primarily due to the

absence of high-resolution tools for evaluating these biomolecular interactions. GlycoMap utilizes methodology developed in the Bertozzi group to metabolically incorporate an azidosialic acid into cell surface glycoproteins using endogenous sialyltransferases.[67] A functionalized Ir photocatalyst can then undergo strain-promoted alkyne-azide cycloaddition (SPAAC), affording Ir-sialylated glycoproteins. Using this method, we first probed hypersialylation in cervical cancer, confirming that HeLa cells exhibited higher sialylation levels compared to primary cervical cells. Analysis of isolated glyco-interactors surprisingly revealed a large number of solute carrier proteins (SLCs) associated with ethanolamine, carnitine, and zinc transport. We validated the functional importance of this interaction by enzymatically depleting sialylic acids and observed differential metabolic intake. Together, our results suggest that cell-surface sialylation and/or interactions with sialylated glycoproteins are associated with SLCs and these may play a crucial role in metabolite transport. Broadly, this strategy demonstrates the utility of metabolic sugar incorporation with proximity labeling as a tool for the discovery of new biological functions of glycosylation. Given that sialic acid is also one of several types of sugar monomers capable of metabolic incorporation strategies, we expect that this experimental workflow will uncover additional biological insights in the coming years.

INTRACELLULAR PHOTOCATALYTIC PROXIMITY LABELING

Although profiling extracellular interactomes is essential for understanding cellular communication and response, intracellular studies are critical for fully elucidating the molecular mechanisms that govern cellular processes. Signaling pathways, gene expression regulation, and organelle function are all highly complex, and proximity labeling has found significant utility for uncovering intracellular dynamics and biomolecular networks. Genetically encoded enzymes, such as peroxidases[20,21] (e.g., engineered ascorbate peroxidase 2 [APEX2], horseradish peroxidase [HRP]) or biotin ligases (e.g., BioID, BASU, TurboID),[18,19,68] are particularly useful as these enzymes are genetically fused to specific targets for mapping protein interactomes in almost any intracellular context. Although photocatalytic proximity labeling exhibits significant advantages in spatiotemporal resolution of tagging, it is inherently more challenging to genetically incorporate photocatalysts into protein targets of interest for intracellular proximity labeling. As such, significant efforts have been devoted to developing biochemical methods to incorporate these materials in the interior of the cellular environment.

Flavin-binding proteins as proximity labeling systems gained initial prominence in the field to rapidly access a genetically encodable system for intracellular labeling. Many of these proteins are derived from naturally occurring photoreceptors, including cryptochromes and phototropins from both plants and photosynthetic cyanobacteria.[69] Phototropins in particular contain a light-sensitive LOV (light, oxygen, voltage) domain that binds a flavin mononucleotide (FMN) prosthetic cofactor (Figure 3A), which endows the protein with the ability to absorb photons upon exposure to light to induce a conformational change.[70] This system is advantageous because all components are endogenously bioavailable and genetically encodable in human cells, and flavin derivatives are widely recognized for their capacities in both electron and energy transfer to generate reactive intermediates (Figure 3B). This property was leveraged to produce reactive oxygen species to enhance observable signals in electron microscopy, wherein researchers engineered and shortened the LOV domain to produce miniSOG (miniature singlet oxygen generator, Figure 3A).[71] Proteins also undergo a variety of chemical reactions in the presence of singlet oxygen,[72] which can be covalently trapped with exogenously added probes. This approach was utilized for mapping subcellular RNA localization patterns using the chromophore-assisted proximity labeling and sequencing platform (CAP-seq)[29] based upon miniSOG oxidation of guanosine residues for subsequent cross-linking with amine-containing probes (Figure 3C).[73,74] Using this method, researchers mapped transcriptomes in different subcellular compartments, including the endoplasmic reticulum and mitochondria, revealing a significant enrichment of messenger RNAs involved in the oxidative phosphorylation pathway at the outer mitochondrial membrane.[29] In parallel, a photoproximity labeling platform was recently developed by the Muir group where they evaluated a range of engineered LOV domains to photolabel nearby proteins following exposure to either a biotin-phenol or biotin-aniline probe. This method, called Light-induced Interactome Tagging (LITag),[54] leverages protein oxidation at certain residues, including oxohistidine which can be covalently trapped with phenol or aniline compounds (Figure 3C). LiTag impressively requires very short labeling times (as little as 1 s irradiation) and has been used to profile a number of systems, including the mitochondrial proteome, poly (ADP-ribose) polymerase 1 (PARP1) interactions following DNA damage, and the interactome of the major vault protein (MVP).[54]

Despite the utility of these systems, singlet oxygen labeling is diffuse (~70–100 nm) and these enzymes are limited to flavin-based catalysts (namely riboflavin or FMN). To increase flexibility in this regard, researchers have expanded this capability by utilizing HaloTag, a modified haloalkane dehalogenase that covalently links a synthetic chloroalkane ligand to a protein of interest (Figure 3D).[75] This tag is flexible and can be appended to fluorophores, purification handles, and catalysts, allowing for self-alkylation installation of almost any payload to a fusion protein in live cells. In addition to employing this technology for Ir photocatalyst installation in our own lab,[76] the Spitale group developed an RNA photoproximity labeling approach (Halo-seq) to uniquely identify transcripts in a subcellular location of interest.[26,27] Chloroalkane-modified bromofluorescein catalysts were installed into various HaloTag fusion proteins, enabling profiling of nuclear, nucleolar and cytoplasmic transcriptomes.

Proximity labeling is especially well-suited to evaluating protein interactions within the nucleus, given that intranuclear interactions are largely transient, multi-valent associations governed by post-translational modifications (PTMs) that intricately coordinate DNA-driven processes.[77,78] In 2022, in collaboration with the Muir group, we developed a genetically encodable μMap technology to incorporate Ir photocatalysts into histone tails to track chromatin state changes in response to cancer mutations.[79] A split intein method utilizing solid-phase peptide synthesis, click chemistry and nucleoprotein *trans*-splicing resulted in site-selective photocatalyst incorporation (Figure 3E). Isolated nuclei from Ir-transfected cells were irradiated with blue light in

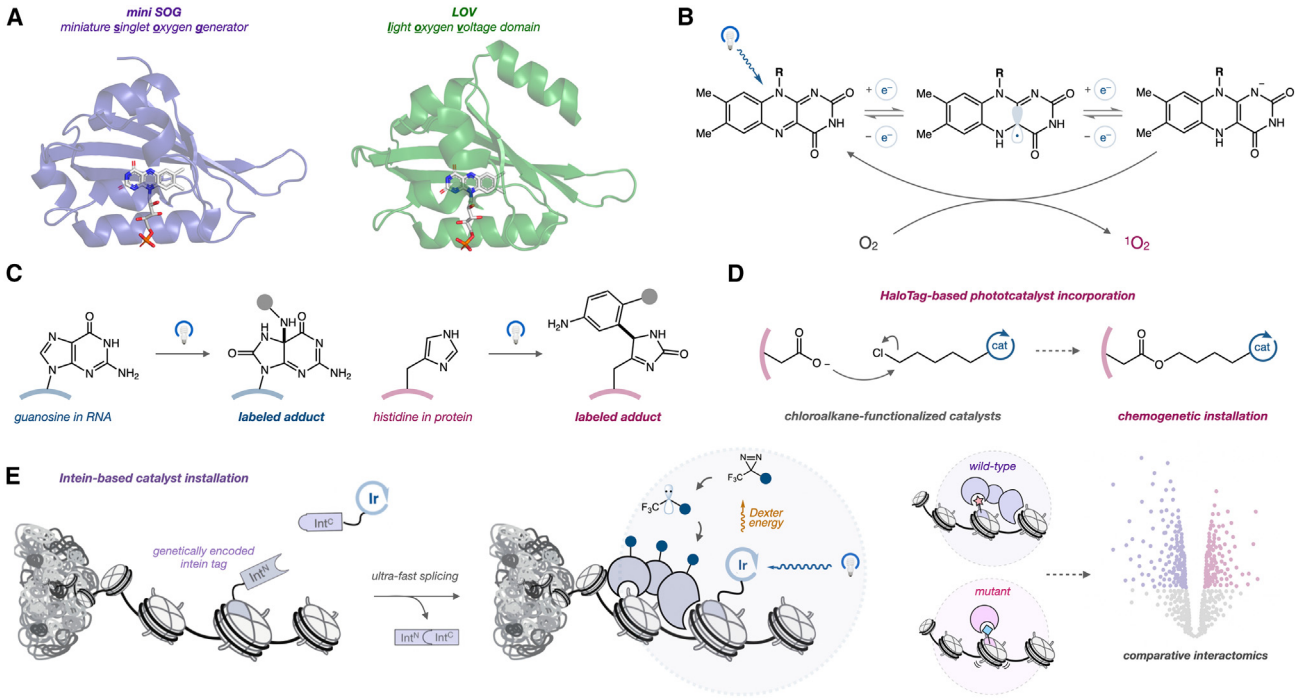

Figure 3. Photocatalytic proximity labeling platforms for intracellular interactome profiling

(A) Two genetically encodable proximity labeling systems, miniSOG (miniature singlet oxygen generator, PDB 6GPU) and LOV (light oxygen voltage domain, PDB 2Z6C) utilize an engineered flavin-binding protein derived from *Arabidopsis thaliana* phototropin 2.

(B) Flavin cofactors generate singlet oxygen ($^1O_2$) through blue light excitation and subsequent energy and/or electron transfer to molecular oxygen.

(C) Photogenerated reactive oxygen species induce oxidation for labeling nucleic acids and proteins with appropriate capture probes.

(D) Photocatalysts can also be chemoenzymatically installed into HaloTag, which self-alkylates molecular payloads containing a chloroalkane linker.

(E) Photocatalyst incorporation facilitated through solid phase peptide synthesis of catalyst-containing inteins, which can undergo *trans*-splicing with a genetically encodable target protein. In this example, Ir photocatalysts were incorporated into histone tails for subsequent μMap profiling of both wild-type and oncohistone mutations for comparative proteomic profiling.

the presence of biotin-diazirine probes to sense local chromatin microenvironment changes in both condensed and open chromatin states. We also examined the H2A E92K mutation, a histone variant associated with various cancer types.[80] In particular, the histone deacetylase SIRT6 was enriched in the wild-type H3, whereas bromodomain (BRD) transcriptional activators BRD2/3/4 were enriched in E92K. These findings suggest that E92K inhibits deacetylase activity, leading to enhanced binding of associated reader proteins. These experiments also revealed a detrimental impact on nucleosomal DNA methyltransferase 3 alpha (DNMT3A) binding upon the introduction of E92K, supporting a model where fewer *de novo* methylation events occur. The ability to probe population-level histone interactomes also motivated us to use μMap for elucidating the functional mechanisms of small molecule ligands within chromatin microenvironments. In particular, we investigated the effect of JQ-1, a BRD inhibitor, on the H2A interactomes. In untreated cells, BRD2/3/4 were all significantly enriched, consistent with the role of JQ-1 role in blocking BRD-nucleosome interactions. Similar experiments were performed with the DOT1L methyltransferase inhibitor, pinometostat, where we support a proposed mechanism that H3 methylation induces recruitment of the acetyltransferase P300, followed by BRD reader recruitment and subsequent transcriptional activation. Together, this study utilized intein-based Ir incorporation into histone tails, and the utility of this nanoscale proximity-labeling method highlights its capacity to uncover crucial alterations in interactomes when confronted with cancer-associated mutations and exposure to small-molecule inhibitors. The implementation of μMap and proximity labeling in epigenetics is likely to enhance our foundational comprehension of nuclear protein-protein interactions, and we anticipate extensive future study in the realm of epigenetic drug discovery.

PHOTOCATALYTIC SMALL MOLECULE TARGET AND BINDING SITE IDENTIFICATION

Photocatalytic proximity labeling has found significant utility in probing the direct (and indirect) protein targets of small molecule drugs (Figure 4A). Traditional methods for target identification (ID) have historically involved appending a photoactivatable group (such as diazirine or phenyl azide) to the molecule of interest to cross-link the molecule to its target protein (Figure 4B).[39,40,81] While there are successful examples of PAL,[82,83] it remains a highly challenging endeavor, chiefly due to the stoichiometric nature of the probe resulting in unproductive reactions with nearby water molecules (Figure 4B). To overcome this inherent challenge, our group, in collaboration with Merck, developed a platform based on the μMap system that utilizes Ir photocatalysts to catalytically activate diazirine molecules, allowing for high resolution and enhanced labeling of small molecule drug targets (Figure 4C).[76] Upon drug-catalyst conjugation, validation experiments are performed to ensure that the

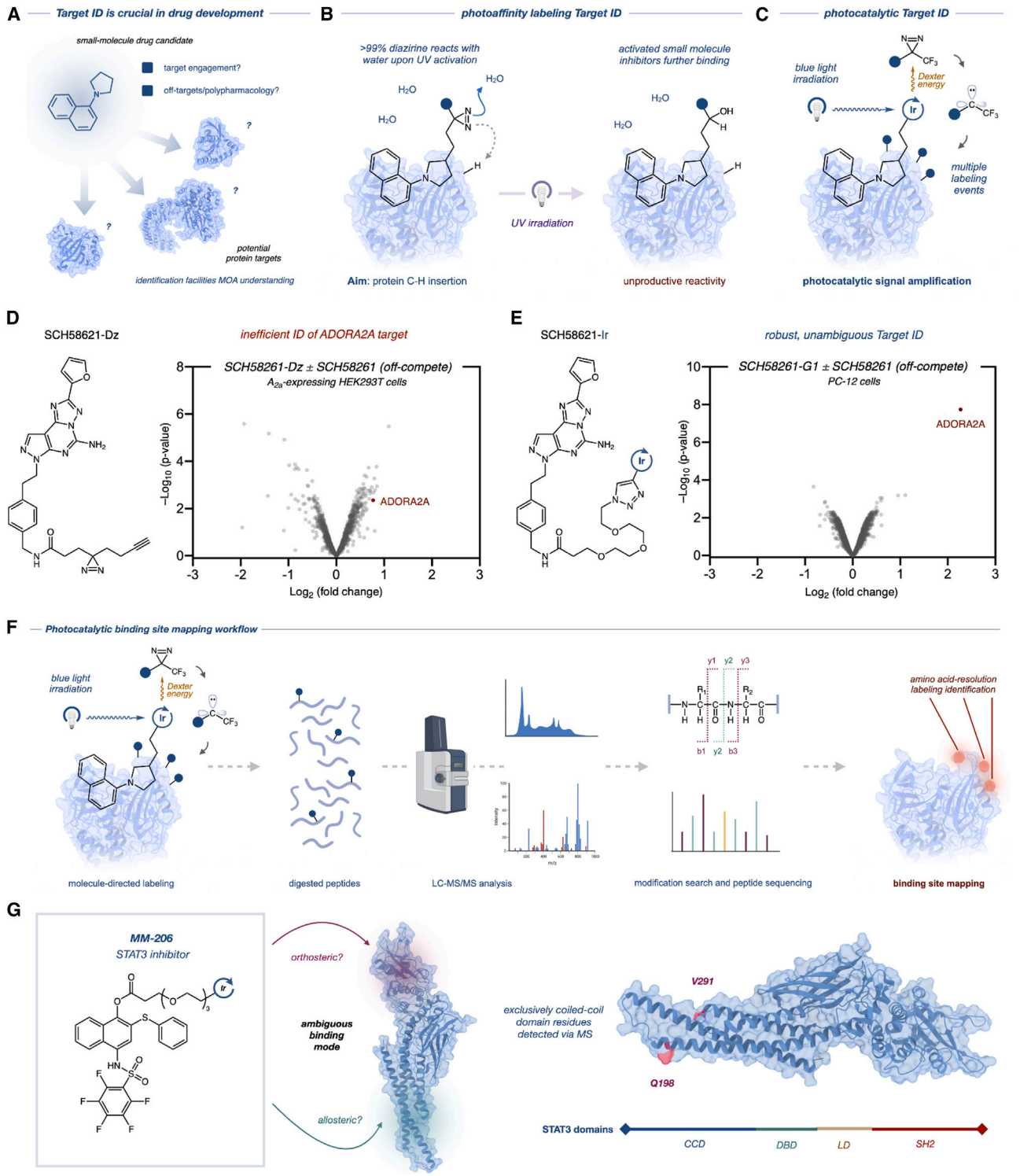

Figure 4. Photocatalytic proximity labeling enhances intracellular target identification and binding site mapping of small molecule drugs

(A) Target and mechanism-of-action identification is key for clinical drug development.

(B) Traditional photoaffinity labeling (PAL) probes utilize stoichiometric identification of targets via UV activation of photocrosslinkers, which predominantly undergo unproductive reactivity with water.

(C) Appending photocatalysts to small molecules enables multiple labeling events to occur on a target of interest, significantly enhancing signal.

(legend continued on next page)

small molecule does not lose its bioactivity or efficacy. The functionally validated drug-Ir conjugate can then bind to its target molecule, and the presence of diazirine-biotin probes leads to labeling of the target under μMap conditions. To initially test the efficacy of this approach, a JQ-1 Ir conjugate was used to identify several BRD protein targets, whereas utilizing the corresponding PAL approach did not yield BRD proteins among any of the top identified candidates. This result demonstrated not only the validity of the approach for target ID, but also the ability to perform successful nuclear labeling, highlighting the permeability of drug-catalyst conjugates and the signal amplification generated via photocatalytic target ID.

This approach was further validated in the context of multiple established therapeutics. In particular, paclitaxel (Taxol), which mechanistically binds to microtubule proteins (tubulins) to disrupt mitosis in a variety of cancers,[84] was synthesized as an Ir conjugate. The μMap ID platform yielded a variety of tubulin proteins via quantitative proteomics, demonstrating effective target ID for chemotherapy agents. μMap ID was also deployed to characterize drugs that exhibit polypharmacology. Specifically, we investigated the kinase inhibitor Dasatinib, which has seen significant clinical and commercial success in the treatment of both chronic myelogenous and acute lymphoblastic leukemia.[85] Dasatinib is an ATP-competitive kinase inhibitor and has been shown to target various kinases, including Src, c-Kit, BCR/Abl, and others.[86] Upon Ir conjugation and labeling, we were able to not only identify various kinase targets, but also key lysosomal off-targets, suggesting a novel subcellular metabolic pathway for kinase inhibitors.[76] Importantly, different kinases were enriched in different cell lines exhibiting either myelogenous or monocytic leukemia phenotypes, highlighting the ability of this approach to provide insight into small molecule polypharmacology in different cellular contexts and disease models. Finally, as a demonstration of the signal amplification afforded by μMap ID, we investigated the ADORA2A-targeting compound SCH58261 as a drug candidate for treating the neurological disorders Parkinson's disease and depression.[87] It is noteworthy that SCH58261 has not been previously amenable to traditional PAL target ID, and our own attempt at isolating ADORA2A via SCH58261-diazirine conjugate yielded inefficient results (Figure 4D). Conversely, μMap ID using an Ir conjugate of SCH58261 substantially improved enrichment of the corresponding G protein-coupled receptor (GPCR) target (Figure 4E), reflecting the catalytic nature of the platform to enhance signal compared to the stoichiometric PAL approach (Figures 4B and 4C).

Having demonstrated μMap as a target-ID platform, we also pursued small molecule binding-site mapping via photocatalysis. In the absence of crystal structure data, binding site determination is an exceedingly challenging endeavor, yet is critical for rational improvements to drug design and mechanistic understanding of drug action. As with target ID, traditional PAL has been used successfully in the past to gain insight into drug binding,[88,89] yet suffers from the signal limitations described previously. We hypothesized that photocatalytic amplification as well as the narrow radius of the carbene generated via μMap could be used to determine sites of insertion on the protein target of interest. Additionally, diazirine-biotin probes have a consistent mass-spec signature which would greatly simplify analysis compared to fragmentation patterns in different complex drug molecules (Figure 4F). Upon demonstrating proof-of-concept on a sulfonamide conjugate that binds carbonic anhydrase, we then illustrated successful binding site mapping on a variety of protein/drug pairs, including kinase inhibitors and molecular glues.[90] We also evaluated MM-206, a weak STAT3-binding molecule with no known binding site (Figure 4G), and were able to unambiguously indicate engagement with the coiled-coil domain of STAT3. Additionally, we were able to perform successful *in cellulo* binding site identification utilizing a JQ1-Ir conjugate, overcoming a long-standing challenge for state-of-the-art methods. Overall, several novel methods that leverage photocatalysis in the pursuit of small-molecule target identification have been developed in recent years. Due to the advantages granted by catalytic turnover of the affinity probe, which greatly increases signal in comparison to traditional stoichiometric methods, these technologies are well-positioned to enable higher fidelity target engagement data for both academic uses and medicinal chemistry development in the clinic.

MEASURING AND MODULATING THE PHOTOCATALYTIC PROXIMITY LABELING RADIUS

Ongoing advances in proximity labeling are producing powerful systems that are more accurate, robust, and versatile. As discussed previously (Figure 1A), the effective labeling radius of a given system is a pivotal parameter influencing the scale and resolution of interactome mapping and is directly determined by the diffusion distance of reactive probes. Enhancing and/or modulating the labeling resolution of proximity labeling platforms is thus crucial for capturing diverse interactome scales. Despite a multitude of photocatalytic proximity labeling systems being developed, there was surprising limited quantitative measurements regarding the actual labeling radii of these various manifolds. To address this question, our group undertook a study to directly measure the resolution of different proximity labeling methods and to investigate the chemical principles governing diffusion of reactive probes in these systems.[32] In order to understand how to influence labeling radius in a proximity labeling platform, we first developed a super-resolution microscopy-based workflow to directly measure the size and distance of labeling events generated with each catalytic manifold. We established a simplified model system for experimentation, consisting of antibody-targeted proximity labeling with each appropriate catalyst on bovine serum albumin (BSA)-coated coverslips, which enables subsequent staining and super-resolution microscopy measurement of labeling events (Figure 5A).

Within this model, we first measured radial clusters of approximately ~50 nm for μMap photocatalytic proximity labeling. This

(D and E) Quantitative chemoproteomic enrichment of ADORA2A with a diazirine-functionalized (D) or iridium catalyst-conjugated (E) SCH58261.
(F) Photocatalytic labeling and mass spectrometry-based workflow for identifying the protein binding site(s) of small molecules.
(G) STAT3 inhibitor MM-206 exhibits an unknown binding mode, which was identified via μMap as an allosteric inhibitor in the coiled-coil domain (CCD) of STAT3 (PDB 6TLC).

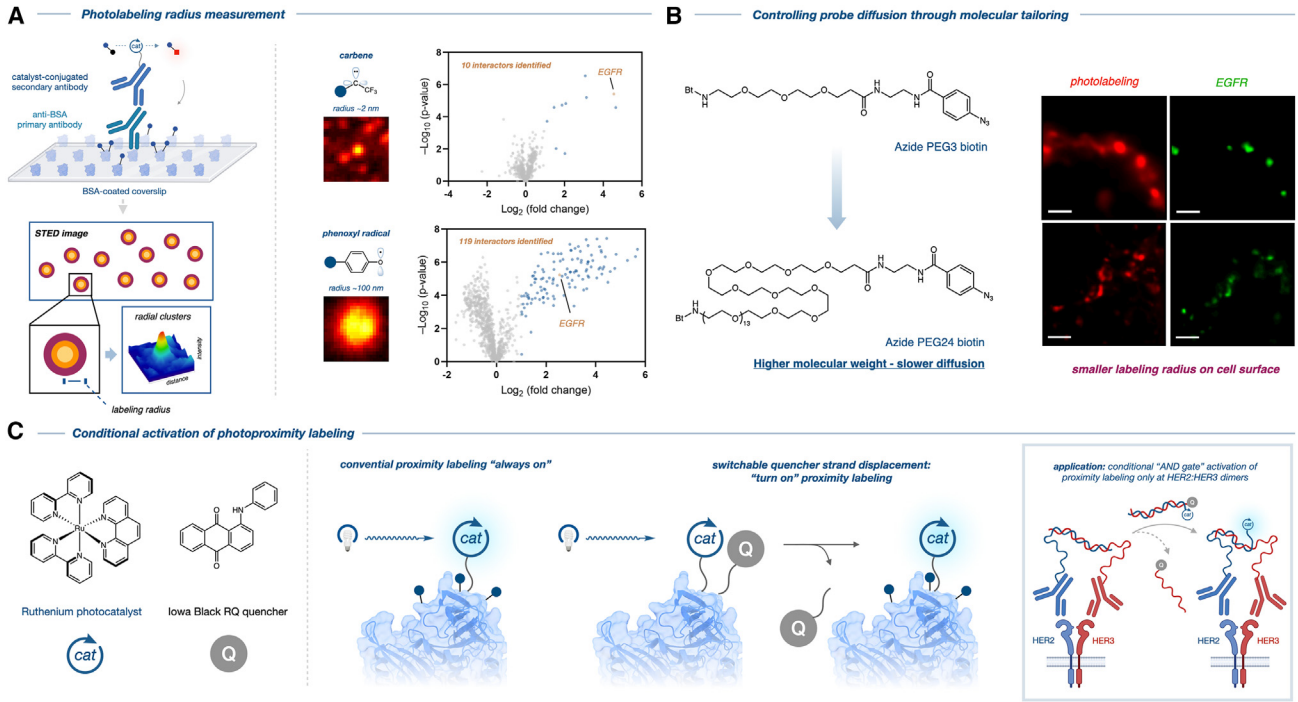

Figure 5. Radius modulation and new controlled activation modes in photocatalytic proximity labeling

(A) The resolution of different proximity labeling systems can be measured *in vitro* using protein-coated glass coverslips and super-resolution microscopy visualization of labeled clusters. Both carbene and phenoxyl radical-based labeling systems were compared in microscopy and quantitative chemoproteomics, illustrating the resolution and spatial selectivity differences with both chemistries.

(B) The diffusion coefficient of reactive species can be adjusted by increasing the molecular weight of probes, resulting in higher resolution labeling as observed by EGFR labeling on the surface of A549 cells.

(C) Photocatalytic proximity labeling can be "activated" through an appropriate quencher coupled with structure-switching DNA aptamers, allowing labeling to occur in user-defined microenvironments.

finding was initially puzzling to us, as μMap generates a reactive carbene probe with a ~1 ns half-life in aqueous solution, resulting in a theoretical labeling radius of approximately 2–4 nm.[34,91] We hypothesized that the use of a dual antibody assembly with a mouse primary BSA antibody followed by a goat anti-mouse Ir-conjugated secondary antibody (Figure 5A) may effectively extend the labeling radius of μMap through the literal size of this assembly (each antibody measures ~15 nm in length).[92] To test this hypothesis, we measured the radius of biotinylation clusters using a goat anti-mouse direct biotin conjugate as secondary antibody in our model BSA system, and indeed observed radial clusters measuring ~50 nm, a value consistent with those obtained with μMap labeling on BSA-coated coverslip and roughly the length of two antibodies.[32,92] In this context, the labeling precision of the μMap protocol is limited by the tether length of the protein-based directing agent (antibodies in this case) and supports a low-nanometer true radius for μMap labeling. Additionally, we measured the labeling resolution of individual peroxidase-based proximity labeling events, which utilize a phenoxyl radical reactive intermediate. In these experiments we accounted for the length of the dual-antibody labeling system and observed a radius of ~100 nm—approximately five times larger than the radius measured for μMap under the same conditions, and consistent with the relative stability of each reactive intermediate (Figure 5A). We also performed quantitative proteomics with both platforms to compare their performance in a proximity labeling experiment targeting epidermal growth factor receptor (EGFR) on the surface of A549 cells. As shown in the volcano plots in Figure 5A, μMap identified EGFR as the most abundant and statistically significant hit along with 10 other proteins corresponding to EGFR interactors. However, in striking contrast to the μMap dataset, the phenoxyl radical-based proximity labeling experiment placed EGFR at the sixty-fourth position in terms of enrichment along with over 100 additional interactors. This outcome aligned with the broader labeling radius using the radical-based probes and reflects the more diffuse biotinylation pattern observed on the cell surface through super-resolution microscopy (Figure 5A). Overall, this report marked the first quantitative comparison of any proximity labeling platform via both microscopy and functional proteomics. We anticipate that this super-resolution method will find utility in benchmarking new proximity labeling platforms as they are developed.

While carbene and phenoxyl radical-based labeling platforms provide complementary spatial resolutions, at the time of our study there was no available proximity labeling platform with an intermediate spatial resolution (between 2 and 100 nm). Development of such a platform would facilitate the investigation of biological structures on the low to mid-micrometer scale, including cell-surface protein clusters in cell adhesion,[93] neurotransmitter signaling,[94] and immunoregulation.[95] To address this technical need, we were intrigued by aryl azides as reactive intermediates. Although these species have been widely

employed in photoaffinity cross-linking,[96] their potential for proximity labeling has only recently been highlighted. Zhang, Chen, and colleagues demonstrated the activation of aryl azide probes using visible light-driven organic photocatalysis.[97] This process involves proposed energy transfer from excited-state photocatalysts to generate aryl nitrene and ketenimine species as reactive probes. We thus explored the possibility of augmenting spatial selectivity through structural modifications of the aryl azide probe. The variations in labeling radii observed across platforms are primarily due to the characteristic half-life of each reactive intermediate. However, we recognized that the species' diffusion coefficient is likely another influential factor in determining the distance traveled by a reactive species in solution. Consequently, we considered the prospect of limiting the labeling radius by diminishing the rate at which the probe can diffuse in solution. In this scenario, the species' half-life would remain constant, but the average distance covered over time would decrease due to reduced diffusion, leading to a higher concentration of localized labeling events and an enhanced spatial resolution. To test this, we lengthened the polyethylene glycol (PEG) linker in the biotin azide probe (Figure 5B), as previous studies have indicated that PEG oligomers exhibit reduced diffusion coefficients with increasing molecular weights.[98] Consequently, we synthesized a PEG_{24} derivative as a diffusion-reduced analog of PEG_3 aryl azide (Figure 5B). Utilizing 2D diffusion ordered nuclear magnetic resonance spectroscopy (DOSYNMR), we observed an approximately 2-fold decrease in the diffusion of the PEG_{24} analog compared to the PEG3 probe,[32] confirming that reduced diffusion can be achieved through this fundamental structural modification.

To assess whether the increased spatial selectivity extends to extracellular microenvironment tagging, we again conducted cell-surface labeling of the EGFR interactome. Aligning with the outcomes observed in our model BSA interactome, we noted significantly smaller labeling clusters for the PEG_{24} aryl azide in comparison to the truncated PEG3 analog (Figure 5B). We also examined the impact of this reduced labeling radius on the enriched extracellular interactome of EGFR. We found that our intermediate-precision PEG_3 aryl azide probe identified 14 enriched proteins, while the higher-precision PEG_{24}-probe exhibited only two significant interactors (ITGA3, PTPRJ), both of which were present in the PEG_3 probe dataset.[32] The convergence between the two analogous datasets indicates that adjusting the diffusion coefficient can permit the capture of concentric interactomes with variable radii. Overall, the diverse aqueous half-lives exhibited by reactive species such as carbenes, nitrenes, and phenoxy radicals offer a complementary array of technologies for interactome mapping. A straightforward approach to fine-tune the labeling radii of these probes involves modulating the diffusion coefficient. We anticipate that this overarching strategy will pave the way for the creation of a spectrum of proximity labeling platforms with varying levels of labeling precision, facilitating the customized mapping of diverse interactomes.

CONDITIONAL ACTIVATION OF PHOTOCATALYTIC LABELING PLATFORMS

In addition to developing new reactive intermediates and photocatalysts for proximity labeling, recent work has investigated new ways to conditionally activate these platforms for additional levels of spatial and temporal control. (Figure 5C) In conventional approaches, a catalyst is targeted to a biomolecule of interest to tag nearby endogenous interactors (Figure 1A). However, traditional approaches operate under the assumption that every microenvironment is identical, thus preventing the application of this technology in subcellular regions that cannot be defined by the location of a single biomolecule of interest. For example, dimerized cell surface receptors are of significant interest because their dysregulation contributes to abnormal cell proliferation, cell survival, and invasion of many cancers.[99] These microenvironments are highly dynamic and unique, and elucidating proteomes proximal to these assemblies could enable the discovery of proteins that are selectively recruited to the dimerized receptors but not their monomeric counterparts. While existing proximity labeling methods have provided valuable biological insights, these photocatalytic manifolds are "always on" upon irradiation, and identifying proteomes with enhanced resolution is conceivable if they could be activated only under certain molecular conditions. The Martell group cleverly addressed this need by developing DNA-based switchable photoproximity catalysts that only become active in the presence of a secondary molecular trigger. These DNA catalysts, composed of a ruthenium photocatalyst and a spectral quencher (Iowa Black RQ) each tethered to a DNA oligomer, are catalytically inert but undergo a conformational change upon encountering a specific molecular trigger, thereby activating proximity labeling at specific microenvironments (Figure 5C).[100]

To develop this powerful system, they selected a heteroleptic $Ru(bpy)_2$(phenanthroline) complex as the photocatalyst, a choice well-informed by their precedent in both proximity labeling and oxidative phenol couplings.[48] More importantly, these complexes exhibit a catalytically active photoexcited state that can be quenched in close proximity to a spectral quencher.[101,102] The switchable system encompasses three key elements: (1) a DNA oligomer undergoing conformational changes in reaction to a molecular trigger, (2) a proximity labeling photocatalyst, and (3) a spectral quencher that deactivates the photocatalyst when they are in close proximity. Initially, the DNA catalyst assumes a conformation where the photocatalyst is inactive due to its proximity to the quencher. However, upon encountering a specific molecular trigger, the DNA undergoes a conformational shift, modifying the distance between the photocatalyst and quencher and triggering the activation of photocatalytic activity (Figure 5C). To construct and validate the switchable DNA proximity labeling catalyst, quencher and Ru single-stranded DNA (ssDNA) oligonucleotide strands were first synthesized and combined to ensure comprehensive quenching. Subsequently, they explored the photocatalytic activity of the DNA catalyst triggered by the presence of a displacement oligonucleotide strand complementary to the loop region of the hairpin sequence, demonstrating ~20-fold increase in activity upon introducing the trigger strand, confirming conditional activation toward an "on" state.[100]

After confirming the capability of the switchable DNA photocatalyst to label proteins *in vitro* only after addition of the ssDNA trigger, the team then extended its application to label proteins on the surface of mammalian cells. With the objective of directing this system to a protein dimer pair, the researchers' initial focus

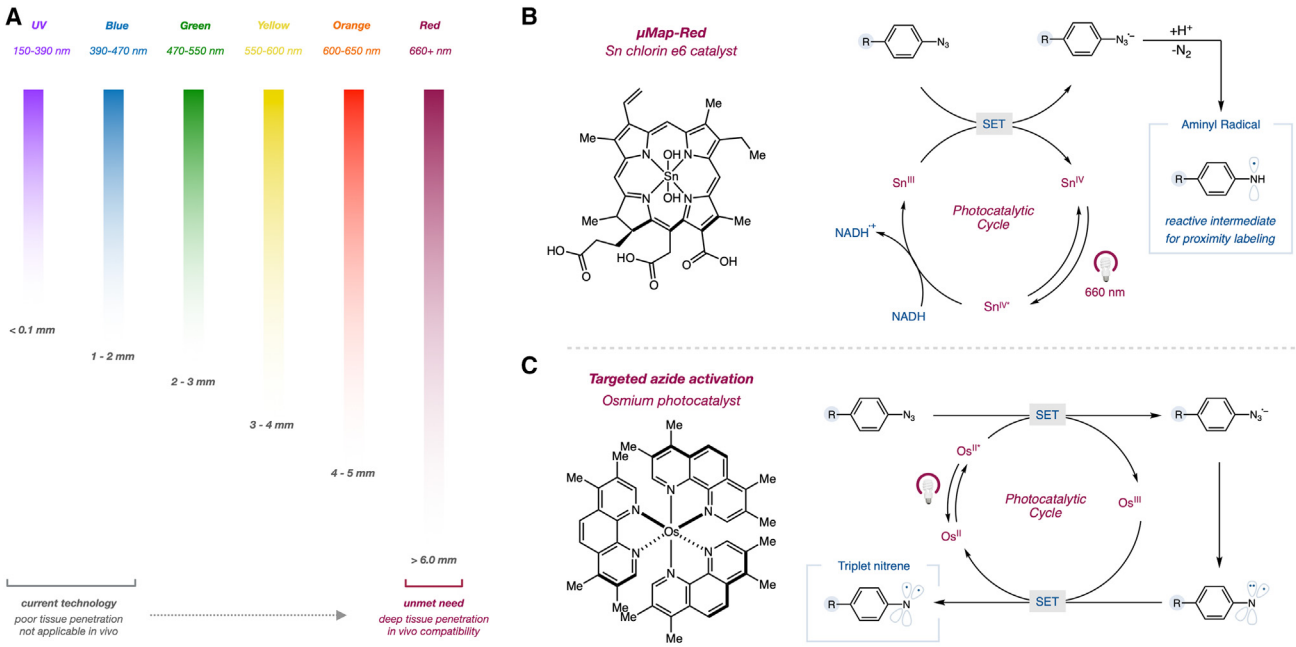

Figure 6. Red-shifted photoredox catalysis modes for proximity labeling

(A) Current activation modes for light-based proximity labeling are shorter in wavelength and exhibit poor tissue penetration. Longer wavelengths of light can address this need for *in vivo* proximity labeling applications.

(B) μMap-Red photocatalytic activation of aryl azides through single electron transfer (SET) to generate aminyl radicals.

(C) Targeted aryl azide activation with osmium photocatalysts through SET to furnish a triplet nitrene reactive intermediate.

was on targeting tyrosine kinase dimers in different heteromeric states (Figure 5C). A dsDNA oligo composed of an invader strand capable of displacing the quencher strand of the Ru-quencher DNA duplex was then engineered, thus activating the photocatalyst only at HER2:HER3 dimer sites, enabling identification of protein-protein interactions associated with increased invasion and growth in certain cancers. Overall, this work represents a significant advance to photocatalytic proximity labeling with the addition of "AND-gate logic" for profiling highly specific microenvironments. Although this study employs a $Ru(bpy)_3$-type complex and biotin phenol protein tagging, the adaptable design of switchable DNA catalysts allows compatibility with almost any synthetic photocatalyst. Additionally, these switchable DNA proximity labeling catalysts can be crafted from conformation-switching DNA aptamers responsive to small molecules, ions, and proteins, paving the way for future applications of photocatalytic proximity labeling in highly specific subcellular locations.

RED LIGHT-ACTIVATED PHOTOCATALYTIC PROXIMITY LABELING

The ability to identify interactions between biomolecules within whole tissues and live animals holds great potential, particularly when studying disease phenotypes. While photocatalytic proximity labeling platforms have been successful in detecting biomolecular interactions in many different cellular contexts, applying these methods *in vivo*, particularly in higher-order mammalian model systems, has proven to be a challenging task. The challenge primarily arises from the presence of natural chromophores in living systems, which limits the effectiveness of activating these labeling systems using shorter wavelengths of light (<500 nm) due to light scattering (Figure 6A).[103] Hence, there has been significant effort devoted to engineering both new reactivity modes as well as distinct photocatalytic platforms that utilize longer wavelengths of light for activation. In nature, porphyrin and chlorin scaffolds serve as prevalent photocatalysts capable of absorbing light in the longer-wavelength range (>600 nm) and channeling this energy into photoinduced electron transfer (ET). Drawing inspiration from these naturally occurring compounds as well as accounts of azide-activating photocatalysts,[104] our group hypothesized that red-light-absorbing catalysts could be harnessed to generate reactive intermediates—specifically nitrenes or aminyl radicals—from aryl azide precursors. This strategy, termed μMap-Red, explored the potential of red light in proximity labeling.[50]

To explore this concept, we first measured conversion of 4-azidobenzoic acid using various red-light photocatalysts with diverse redox properties. Employing a tin (Sn)-metalated chlorin e6 catalyst, we observed minimal conversion (5%) and slight formation of the aniline product 2 (2%). Significantly enhanced yields were achieved with the addition of stoichiometric reductants, such as glutathione, sodium ascorbate, or nicotinamide adenine dinucleotide (NADH), with NADH proving most effective (83% yield). Based on these results, we proposed a mechanistic pathway initiated by the reductive quenching of the excited-state photocatalyst with NADH, forming a highly reducing organic ground state. This reduced species is then poised for single electron transfer (SET) to the aryl azide, effectively regenerating the catalyst. Mesolytic cleavage of the azide radical anion releases molecular nitrogen,

and rapid protonation reveals an aminyl radical species as a reactive intermediate for proximity labeling (Figure 6B). Ultrafast transient-absorption spectroscopy supported the proposed mechanism by demonstrating that the excited Sn-chlorin catalyst is quenched by NADH and not by the aryl azide.[50]

With a system for red-light activation of aryl azides in place, we tested μMap-Red in a cellular context. By using a primary antibody specific to EGFR, a Sn-chlorin e6 conjugated secondary antibody, and red-light irradiation, we successfully labeled the cell surface microenvironment of EGFR on A549 cells. Quantitative proteomics analysis revealed statistically significant enrichment of previously validated physical interactions with EGFR, including CD44, AXL, EPHA2, and EPHB2. Our next step was to evaluate μMap-Red in a complex biological sample where blue-light activation was not feasible. Whole blood, with its high biochemical complexity, served as our testing ground to assess whether μMap-Red could enable selective proximity labeling. We selected TER119, an antibody specific to mature red blood cells.[105] While TER119 is highly selective for erythrocytes, it has been shown to bind to several targets on red blood cells.[106] Using a Sn-chlorin conjugated antibody to TER119, we successfully enriched several candidate erythrocyte proteins, likely representing the antigens recognized by TER119. Importantly, an Ir-conjugated TER119 antibody was unable to yield sufficient labeling in whole blood, reflecting the poor penetration of blue light in complex biological settings containing various endogenous chromophores.

In parallel to μMap-Red, the Rovis group developed a complementary red light-based photocatalytic proximity labeling system (Figure 6C).[52] Initially designed for chemical transformations, these systems utilize osmium (Os)-based photocatalysts, which offer superior light absorption and scalability.[107] Leveraging these red light-based platforms for photoredox catalysis, the Rovis group developed a red-light-activated photocatalytic proximity labeling platform composed of an Os photocatalyst combined with a tetrafluorophenyl azide probe to generate reactive triplet nitrenes (Figure 6C). Density functional theory (DFT) calculations were performed to elucidate the potential mechanism for obtaining the triplet nitrene. EnT was ruled out as a viable pathway, given that the required vertical and adiabatic singlet-to-triplet energies for obtaining the triplet azide exceeded that of the Os photocatalyst.[108] In contrast, an ET mechanism was found to be energetically favorable, with the reduced azide being highly stabilized through both solvation and fluorination. The researchers also observed that the barrier to N_2 dissociation upon reduction was minimal, and N_2 loss as highly exothermic. Subsequent exothermic re-oxidation of the reduced nitrene then generates the triplet nitrene, suggesting a photoredox-catalyzed, stepwise reduction-dissociation-oxidation pathway (Figure 6C). With this platform, the group then explored the protein microenvironment of epithelial cell adhesion molecule (EpCAM) on HCT116 cells within three distinct cell systems: cells cultivated in monoculture and detached in single-cell suspension, cells grown in 3D spheroid culture, and dissociated cells from mouse tumor xenograft tissue. In each of these cell systems, EpCAM-targeted biotinylation was performed using a dual antibody system with Os-conjugated secondary antibodies, followed by enrichment and quantitation using tandem mass tag (TMT)-based liquid chromatography-tandem mass spectrometry (LC-MS/MS) proteomic analysis. EpCAM was consistently detected as highly enriched in each of the cell systems, confirming the efficacy of the technology in labeling and enriching the targeted protein.[52] Overall, the devised photoredox strategy to generate high-energy nitrenes using low-energy light through a redox-neutral ET process represents a significant chemical advance for photocatalytic proximity labeling. We anticipate that this mode of triplet nitrene activation will also uncover new chemical reactivity and attract new applications for synthesis and chemical biology. Together, μMap-Red and the Os-based systems developed by the Rovis group represent significant advancements in the field of photocatalytic proximity labeling, particularly in the utilization of lower-energy red light that exhibits improved tissue penetration. Both platforms are highly modular and can be directed to targets of interest through a variety of means, and we expect that these platforms will find broad applications in interactome profiling in tissues and, eventually, in whole vertebrate animal models.

DISCUSSION

The future is bright for photocatalytic proximity labeling. Over the past decade, the field has grown substantially, and a variety of different platforms have been successfully developed and implemented (Table 1). Despite these successes, the field is still young, and significant challenges remain to engineer and adopt these technologies across all biological settings. From a fundamental standpoint, both standardization and accessibility are needed to fully realize the potential of photocatalytic proximity labeling. Streamlining tool development and deployment is likely to accelerate the adoption of these platforms across various research areas. This will be especially true for potential clinical applications attempting to understand disease-specific interactomes from primary patient samples. The potential of light-activated proximity labeling as a point-of-use diagnostic in various disease stages could pave the way for an unprecedented level of precision personalized medicine. However, with the increasing complexity of data generated by these labeling experiments, there is a need for robust and standardized workflows for data analysis and computational processing. Future opportunities lie in developing user-friendly software that can handle large datasets, extract meaningful information, and facilitate rapid interpretation. Merging these datasets with artificial intelligence systems and language learning models also holds great potential for quickly gaining biological insight from dense interactomic data.

On the technical side, many opportunities remain for improving existing systems or developing entirely new chemistry for photocatalytic proximity labeling. There is continued need for further catalyst engineering and incorporation strategies, whether genetic or otherwise, to facilitate efficient protein profiling in various environments with minimal disruption. In particular, the intrinsic affinity of different photocatalysts toward cellular organelles is a key parameter for their successful application in biological systems. It is known that Ir-based catalysts exhibit inherent affinity toward mitochondria and the endoplasmic reticulum,[37,109] yet the precise chemical principles

governing this affinity are not well understood and many other catalytic systems remain uncharacterized. Further delineation of these factors will enable the development of more efficient and less invasive proximity labeling systems, particularly in live cell and eventual or *in vivo* experiments. Similarly, there is a need for new reactive probes that are more robust, sensitive, tunable, and compatible in a variety of biological settings. For example, enhancing the temporal resolution and compatibility of photocatalytic labeling experiments with live-cell imaging remains problematic. Overcoming this hurdle would enable dynamic tracking of protein interactions in real-time within living cells, providing valuable insights into temporal aspects of cellular processes. Expanding the multiplexing capabilities of photocatalytic proximity labeling would also allow powerful simultaneous profiling of multiple biomolecular interactions. Developing methods to selectively activate different orthogonal probes in a spatially and temporally controlled manner could unlock new dimensions in interactome mapping while minimizing material and variance from multiple experiments. Similarly, design of probes with tuned chemoselectivity for a specific microenvironment state, including specific post-translation modifications, would be an enabling technology for understanding the biological consequences of these events. Continued work toward designing such ''conditional'' or ''turn on'' proximity labeling systems will also find broad utility in profiling variable microenvironments with user defined criteria (time, molecular composition, temperature, ion concentration, etc). Integrating photoproximity labeling with other omics technologies, such as genomics, transcriptomics, and metabolomics, would also provide a more comprehensive view of cellular processes. This type of interdisciplinary approach could uncover intricate regulatory networks and signaling pathways. Proximity labeling and photocatalysis also hold great potential for site-specific modification and engineering of proteins. Integrating catalysts into specific amino acid residues could enable selective modification and mutation of individual residues or regions to yield new biotherapeutics or research tools. Lastly, while promising initial work has been made toward *in vivo* applications with red light-activated systems, these wavelengths still do not fully penetrate deep tissue (>10 mm) and there remains to be a full demonstration of live animal *in vivo* photocatalytic proximity labeling to date in higher mammals. A true long-wavelength photolabeling approach amenable to very deep tissue penetration would prove immensely valuable for studying proteins in their most native environment.

ACKNOWLEDGMENTS

The authors are grateful for financial support provided by the National Institute of General Medical Sciences of the National Institutes of Health (R35GM134897), the Princeton Catalysis Initiative, and kind gifts from Merck, Janssen, BMS, Genentech, Genmab, and Pfizer. S.D.K. acknowledges the NIH for a postdoctoral fellowship (1F32GM142206).

DECLARATION OF INTERESTS

D.W.C.M. declares an ownership interest in the company Dexterity Pharma LLC, which has commercialized materials used in this work. D.W.C.M. is an inventor on patents 20230100536 and 20220306683. D.W.C.M., S.D.K., and B.F.B. are inventors on provisional patent 63/428,899. D.W.C.M. and S.D.K. are inventors on provisional patent 63/419,519. D. W.C.M., S.D.K., and S.W.H. are inventors on provisional patent 63/424,581.

REFERENCES

1. Keskin, O., Tuncbag, N., and Gursoy, A. (2016). Predicting protein–protein interactions from the molecular to the proteome level. Chemical reviews *116*, 4884–4909.

2. Bludau, I., and Aebersold, R. (2020). Proteomic and interactomic insights into the molecular basis of cell functional diversity. Nat. Rev. Mol. Cell Biol. *21*, 327–340.

3. Hentze, M.W., Castello, A., Schwarzl, T., and Preiss, T. (2018). A brave new world of RNA-binding proteins. Nat. Rev. Mol. Cell Biol. *19*, 327–341.

4. Hershfinkel, M., Moran, A., Grossman, N., and Sekler, I. (2001). A zinc-sensing receptor triggers the release of intracellular Ca2+ and regulates ion transport. Proc. Natl. Acad. Sci. USA *98*, 11749–11754.

5. Casey, J.R., Grinstein, S., and Orlowski, J. (2010). Sensors and regulators of intracellular pH. Nat. Rev. Mol. Cell Biol. *11*, 50–61.

6. Murakami, A., Nagao, K., Sakaguchi, R., Kida, K., Hara, Y., Mori, Y., Okabe, K., Harada, Y., and Umeda, M. (2022). Cell-autonomous control of intracellular temperature by unsaturation of phospholipid acyl chains. Cell Rep. *38*.

7. Webster, M.W., and Weixlbaumer, A. (2021). The intricate relationship between transcription and translation. Proc. Natl. Acad. Sci. USA *118*, e2106284118.

8. Huberman, J.A., and Riggs, A.D. (1968). On the mechanism of DNA replication in mammalian chromosomes. Journal of molecular biology *32*, 327–341.

9. Hicks, K.G., Cluntun, A.A., Schubert, H.L., Hackett, S.R., Berg, J.A., Leonard, P.G., Ajalla Aleixo, M.A., Zhou, Y., Bott, A.J., Salvatore, S.R., et al. (2023). Protein-metabolite interactomics of carbohydrate metabolism reveal regulation of lactate dehydrogenase. Science *379*, 996–1003.

10. Wagner, J.P., Wolf-Yadlin, A., Sevecka, M., Grenier, J.K., Root, D.E., Lauffenburger, D.A., and MacBeath, G. (2013). Receptor tyrosine kinases fall into distinct classes based on their inferred signaling networks. Sci. Signal. *6*, ra58.

11. Andrei, S.A., Sijbesma, E., Hann, M., Davis, J., O'Mahony, G., Perry, M.W.D., Karawajczyk, A., Eickhoff, J., Brunsveld, L., Doveston, R.G., et al. (2017). Stabilization of protein-protein interactions in drug discovery. Expert Opin. Drug Discov. *12*, 925–940.

12. Bonifacino, J.S., Dell'Angelica, E.C., and Springer, T.A. (1999). Immunoprecipitation. Curr. Protoc. Protein Sci. *18*, 9.8.1–9.8.28.

13. Lindenmann, J., and Klein, P.A. (1964). Mouse Tissue Isoantigen Detectable by Immunoprecipitation. PSEBM (Proc. Soc. Exp. Biol. Med.) *117*, 446–449.

14. Free, R.B., Hazelwood, L.A., and Sibley, D.R. (2009). Identifying novel protein-protein interactions using co-immunoprecipitation and mass spectroscopy. Current protocols in neuroscience *46*, 5.28.21–25.28.14.

15. Luo, Y., Batalao, A., Zhou, H., and Zhu, L. (1997). Mammalian two-hybrid system: a complementary approach to the yeast two-hybrid system. Biotechniques *22*, 350–352.

16. Qin, W., Cho, K.F., Cavanagh, P.E., and Ting, A.Y. (2021). Deciphering molecular interactions by proximity labeling. Nat. Methods *18*, 133–143.

17. Seath, C.P., Trowbridge, A.D., Muir, T.W., and MacMillan, D.W.C. (2021). Reactive intermediates for interactome mapping. Chem. Soc. Rev. *50*, 2911–2926.

18. Kwon, K., and Beckett, D. (2000). Function of a conserved sequence motif in biotin holoenzyme synthetases. Protein Sci. *9*, 1530–1539.

19. Roux, K.J., Kim, D.I., Raida, M., and Burke, B. (2012). A promiscuous biotin ligase fusion protein identifies proximal and interacting proteins in mammalian cells. Journal of cell biology *196*, 801–810.

20. Rhee, H.-W., Zou, P., Udeshi, N.D., Martell, J.D., Mootha, V.K., Carr, S.A., and Ting, A.Y. (2013). Proteomic mapping of mitochondria in living cells via spatially restricted enzymatic tagging. Science *339*, 1328–1331.

21. Martell, J.D., Deerinck, T.J., Sancak, Y., Poulos, T.L., Mootha, V.K., Sosinsky, G.E., Ellisman, M.H., and Ting, A.Y. (2012). Engineered ascorbate peroxidase as a genetically encoded reporter for electron microscopy. Nat. Biotechnol. *30*, 1143–1148.

22. Fancy, D.A., and Kodadek, T. (1999). Chemistry for the analysis of protein–protein interactions: rapid and efficient cross-linking triggered by long wavelength light. Proc. Natl. Acad. Sci. USA *96*, 6020–6024.

23. Sato, S., Morita, K., and Nakamura, H. (2015). Regulation of target protein knockdown and labeling using ligand-directed Ru (bpy) 3 photocatalyst. Bioconjug. Chem. *26*, 250–256.

24. Baier, J., Maisch, T., Maier, M., Engel, E., Landthaler, M., and Bäumler, W. (2006). Singlet oxygen generation by UVA light exposure of endogenous photosensitizers. Biophys. J. *91*, 1452–1459.

25. Lynch, P.G., Richards, H., and Wustholz, K.L. (2019). Unraveling the Excited-State Dynamics of Eosin Y Photosensitizers Using Single-Molecule Spectroscopy. J. Phys. Chem. A *123*, 2592–2600.

26. Engel, K.L., Lo, H.-Y.G., Goering, R., Li, Y., Spitale, R.C., and Taliaferro, J.M. (2022). Analysis of subcellular transcriptomes by RNA proximity labeling with Halo-seq. Nucleic acids research *50*, e24.

27. Lo, H.Y.G., Engel, K.L., Goering, R., Li, Y., Spitale, R.C., and Taliaferro, J.M. (2022). Halo-seq: An RNA Proximity Labeling Method for the Isolation and Analysis of Subcellular RNA Populations. Current Protocols *2*, e424.

28. Ding, T., Zhu, L., Fang, Y., Liu, Y., Tang, W., and Zou, P. (2020). Chromophore-Assisted Proximity Labeling of DNA Reveals Chromosomal Organization in Living Cells. Angew. Chem. Int. Ed. *59*, 22933–22937.

29. Wang, P., Tang, W., Li, Z., Zou, Z., Zhou, Y., Li, R., Xiong, T., Wang, J., and Zou, P. (2019). Mapping spatial transcriptome with light-activated proximity-dependent RNA labeling. Nat. Chem. Biol. *15*, 1110–1119.

30. Zhai, Y., Huang, X., Zhang, K., Huang, Y., Jiang, Y., Cui, J., Zhang, Z., Chiu, C.K.C., Zhong, W., and Li, G. (2022). Spatiotemporal-resolved protein networks profiling with photoactivation dependent proximity labeling. Nat. Commun. *13*, 4906.

31. Zheng, F., Yu, C., Zhou, X., and Zou, P. (2023). Genetically encoded photocatalytic protein labeling enables spatially-resolved profiling of intracellular proteome. Nat. Commun. *14*, 2978.

32. Oakley, J.V., Buksh, B.F., Fernández, D.F., Oblinsky, D.G., Seath, C.P., Geri, J.B., Scholes, G.D., and MacMillan, D.W.C. (2022). Radius measurement via super-resolution microscopy enables the development of a variable radii proximity labeling platform. Proc. Natl. Acad. Sci. USA *119*. e2203027119.

33. Sies, H. (1993). Strategies of antioxidant defense. Eur. J. Biochem. *215*, 213–219.

34. Geri, J.B., Oakley, J.V., Reyes-Robles, T., Wang, T., McCarver, S.J., White, C.H., Rodriguez-Rivera, F.P., Parker, D.L., Jr., Hett, E.C., Fadeyi, O.O., Oslund, R.C., and MacMillan, D.W.C. (2020). Microenvironment mapping via Dexter energy transfer on immune cells. Science *367*, 1091–1097.

35. Liu, J., Cai, L., Sun, W., Cheng, R., Wang, N., Jin, L., Rozovsky, S., Seiple, I.B., and Wang, L. (2019). Photocaged quinone methide crosslinkers for light-controlled chemical crosslinking of protein–protein and protein–DNA complexes. Angew. Chem. Int. Ed. *58*, 18839–18843.

36. Liu, J., Li, S., Aslam, N.A., Zheng, F., Yang, B., Cheng, R., Wang, N., Rozovsky, S., Wang, P.G., Wang, Q., and Wang, L. (2019). Genetically encoding photocaged quinone methide to multitarget protein residues covalently in vivo. J. Am. Chem. Soc. *141*, 9458–9462.

37. Huang, Z., Liu, Z., Xie, X., Zeng, R., Chen, Z., Kong, L., Fan, X., and Chen, P.R. (2021). Bioorthogonal photocatalytic decaging-enabled mitochondrial proteomics. J. Am. Chem. Soc. *143*, 18714–18720.

38. Liu, Z., Xie, X., Huang, Z., Lin, F., Liu, S., Chen, Z., Qin, S., Fan, X., and Chen, P.R. (2022). Spatially resolved cell tagging and surfaceome labeling via targeted photocatalytic decaging. Chem *8*, 2179–2191.

39. Das, J. (2011). Aliphatic diazirines as photoaffinity probes for proteins: recent developments. Chemical reviews *111*, 4405–4417.

40. Smith, E., and Collins, I. (2015). Photoaffinity labeling in target-and binding-site identification. Future Med. Chem. *7*, 159–183.

41. Hermanson, G.T. (2013). Bioconjugate Techniques (Academic press).

42. Gandhi, L., Rodríguez-Abreu, D., Gadgeel, S., Esteban, E., Felip, E., De Angelis, F., Domine, M., Clingan, P., Hochmair, M.J., Powell, S.F., et al. (2018). Pembrolizumab plus chemotherapy in metastatic non–small-cell lung cancer. N. Engl. J. Med. *378*, 2078–2092.

43. Oslund, R.C., Reyes-Robles, T., White, C.H., Tomlinson, J.H., Crotty, K.A., Bowman, E.P., Chang, D., Peterson, V.M., Li, L., Frutos, S., et al. (2022). Detection of cell–cell interactions via photocatalytic cell tagging. Nat. Chem. Biol. *18*, 850–858.

44. Müller, M., Gräbnitz, F., Barandun, N., Shen, Y., Wendt, F., Steiner, S.N., Severin, Y., Vetterli, S.U., Mondal, M., and Prudent, J.R. (2021). Light-mediated discovery of surfaceome nanoscale organization and intercellular receptor interaction networks. Nat. Commun. *12*, 7036.

45. Achour, A., Michaëlsson, J., Harris, R.A., Odeberg, J., Grufman, P., Sandberg, J.K., Levitsky, V., Kärre, K., Sandalova, T., and Schneider, G. (2002). A structural basis for LCMV immune evasion: subversion of H-2Db and H-2Kb presentation of gp33 revealed by comparative crystal structure analyses. Immunity *17*, 757–768.

46. Chen, L., and Flies, D.B. (2013). Molecular mechanisms of T cell co-stimulation and co-inhibition. Nat. Rev. Immunol. *13*, 227–242.

47. Bolton, J. (2014). Quinone methide bioactivation pathway: contribution to toxicity and/or cytoprotection? Curr. Org. Chem. *18*, 61–69.

48. Nakane, K., Sato, S., Niwa, T., Tsushima, M., Tomoshige, S., Taguchi, H., Ishikawa, M., and Nakamura, H. (2021). Proximity histidine labeling by umpolung strategy using singlet oxygen. J. Am. Chem. Soc. *143*, 7726–7731.

49. Hope, T.O., Reyes-Robles, T., Ryu, K.A., Mauries, S., Removski, N., Maisonneuve, J., Oslund, R.C., Fadeyi, O.O., and Frenette, M. (2023). Targeted proximity-labelling of protein tyrosines via flavin-dependent photoredox catalysis with mechanistic evidence for a radical–radical recombination pathway. Chem. Sci. *14*, 7327–7333.

50. Buksh, B.F., Knutson, S.D., Oakley, J.V., Bissonnette, N.B., Oblinsky, D.G., Schwoerer, M.P., Seath, C.P., Geri, J.B., Rodriguez-Rivera, F.P., Parker, D.L., et al. (2022). μMap-Red: Proximity Labeling by Red Light Photocatalysis. J. Am. Chem. Soc. *144*, 6154–6162.

51. Wagner, B.D., Ruel, G., and Lusztyk, J. (1996). Absolute kinetics of aminium radical reactions with olefins in acetonitrile solution1. J. Am. Chem. Soc. *118*, 13–19.

52. Tay, N.E.S., Ryu, K.A., Weber, J.L., Olow, A.K., Cabanero, D.C., Reichman, D.R., Oslund, R.C., Fadeyi, O.O., and Rovis, T. (2023). Targeted activation in localized protein environments via deep red photoredox catalysis. Nat. Chem. *15*, 101–109.

53. Reiser, A., Willets, F., Terry, G., Williams, V., and Marley, R. (1968). Photolysis of aromatic azides. Part 4.—Lifetimes of aromatic nitrenes and absolute rates of some of their reactions. Trans. Faraday Soc. *64*, 3265–3275.

54. Hananya, N., Ye, X., Koren, S., and Muir, T.W. (2023). A genetically encoded photoproximity labeling approach for mapping protein territories. Proc. Natl. Acad. Sci. USA *120*. e2219339120.

55. Suzuki, S., Geri, J.B., Knutson, S.D., Bell-Temin, H., Tamura, T., Fernández, D.F., Lovett, G.H., Till, N.A., Heller, B.L., Guo, J., et al. (2022). Photochemical Identification of Auxiliary Severe Acute Respiratory Syndrome Coronavirus 2 Host Entry Factors Using μMap. J. Am. Chem. Soc. *144*, 16604–16611.

56. Datta, S., Chen, D.-Y., Tavares, A.H., Reyes-Robles, T., Ryu, K.A., Khan, N., Bechtel, T.J., Bertoch, J.M., White, C.H., Hazuda, D.J., et al. (2023). High-resolution photocatalytic mapping of SARS-CoV-2 spike interactions on the cell surface. Cell Chem. Biol. *30*, 1313–1322.e7.

57. Huang, M.L., Tota, E.M., Lucas, T.M., and Godula, K. (2018). Influencing Early Stages of Neuromuscular Junction Formation through Glycocalyx Engineering. ACS Chem. Neurosci. *9*, 3086–3093.

58. Purcell, S.C., and Godula, K. (2019). Synthetic glycoscapes: addressing the structural and functional complexity of the glycocalyx. Interface Focus *9*, 20180080.

59. Zanetta, J.P., Kuchler, S., Lehmann, S., Badache, A., Maschke, S., Thomas, D., Dufourcq, P., and Vincendon, G. (1992). Glycoproteins and lectins in cell adhesion and cell recognition processes. Histochem. J. *24*, 791–804.

60. An, H.J., Froehlich, J.W., and Lebrilla, C.B. (2009). Determination of glycosylation sites and site-specific heterogeneity in glycoproteins. Curr. Opin. Chem. Biol. *13*, 421–426.

61. Reily, C., Stewart, T.J., Renfrow, M.B., and Novak, J. (2019). Glycosylation in health and disease. Nat. Rev. Nephrol. *15*, 346–366.

62. Meyer, C.F., Seath, C.P., Knutson, S.D., Lu, W., Rabinowitz, J.D., and MacMillan, D.W.C. (2022). Photoproximity Labeling of Sialylated Glycoproteins (GlycoMap) Reveals Sialylation-Dependent Regulation of Ion Transport. J. Am. Chem. Soc. *144*, 23633–23641.

63. Dobie, C., and Skropeta, D. (2021). Insights into the role of sialylation in cancer progression and metastasis. Br. J. Cancer *124*, 76–90.

64. Gray, M.A., Stanczak, M.A., Mantuano, N.R., Xiao, H., Pijnenborg, J.F.A., Malaker, S.A., Miller, C.L., Weidenbacher, P.A., Tanzo, J.T., Ahn, G., et al. (2020). Targeted glycan degradation potentiates the anticancer immune response in vivo. Nat. Chem. Biol. *16*, 1376–1384.

65. Renkonen, J., Paavonen, T., and Renkonen, R. (1997). Endothelial and epithelial expression of sialyl Lewis(x) and sialyl Lewis(a) in lesions of breast carcinoma. Int. J. Cancer *74*, 296–300.

66. Shiozaki, K., Yamaguchi, K., Takahashi, K., Moriya, S., and Miyagi, T. (2011). Regulation of sialyl Lewis antigen expression in colon cancer cells by sialidase NEU4. J. Biol. Chem. *286*, 21052–21061.

67. Dube, D.H., and Bertozzi, C.R. (2003). Metabolic oligosaccharide engineering as a tool for glycobiology. Curr. Opin. Chem. Biol. *7*, 616–625.

68. Branon, T.C., Bosch, J.A., Sanchez, A.D., Udeshi, N.D., Svinkina, T., Carr, S.A., Feldman, J.L., Perrimon, N., and Ting, A.Y. (2018). Efficient proximity labeling in living cells and organisms with TurboID. Nat. Biotechnol. *36*, 880–887.

69. Losi, A. (2007). Flavin-based blue-light photosensors: a photobiophysics update. Photochem. Photobiol. *83*, 1283–1300.

70. Christie, J.M., Salomon, M., Nozue, K., Wada, M., and Briggs, W.R. (1999). LOV (light, oxygen, or voltage) domains of the blue-light photoreceptor phototropin (nph1): binding sites for the chromophore flavin mononucleotide. Proc. Natl. Acad. Sci. USA *96*, 8779–8783.

71. Shu, X., Lev-Ram, V., Deerinck, T.J., Qi, Y., Ramko, E.B., Davidson, M.W., Jin, Y., Ellisman, M.H., and Tsien, R.Y. (2011). A genetically encoded tag for correlated light and electron microscopy of intact cells, tissues, and organisms. PLoS Biol. *9*, e1001041.

72. Davies, M.J. (2004). Reactive species formed on proteins exposed to singlet oxygen. Photochem. Photobiol. Sci. *3*, 17–25.

73. Xu, X., Muller, J.G., Ye, Y., and Burrows, C.J. (2008). DNA− protein cross-links between guanine and lysine depend on the mechanism of oxidation for formation of C5 vs C8 guanosine adducts. J. Am. Chem. Soc. *130*, 703–709.

74. Ding, Y., Fleming, A.M., and Burrows, C.J. (2017). Sequencing the mouse genome for the oxidatively modified base 8-oxo-7, 8-dihydroguanine by OG-Seq. J. Am. Chem. Soc. *139*, 2569–2572.

75. Los, G.V., Encell, L.P., McDougall, M.G., Hartzell, D.D., Karassina, N., Zimprich, C., Wood, M.G., Learish, R., Ohana, R.F., Urh, M., et al. (2008). HaloTag: a novel protein labeling technology for cell imaging and protein analysis. ACS Chem. Biol. *3*, 373–382.

76. Trowbridge, A.D., Seath, C.P., Rodriguez-Rivera, F.P., Li, B.X., Dul, B.E., Schwaid, A.G., Buksh, B.F., Geri, J.B., Oakley, J.V., Fadeyi, O.O., et al. (2022). Small molecule photocatalysis enables drug target identification via energy transfer. Proc. Natl. Acad. Sci. USA *119*, e2208077119.

77. Kouzarides, T. (2007). Chromatin modifications and their function. Cell *128*, 693–705.

78. Ruffner, H., Bauer, A., and Bouwmeester, T. (2007). Human protein-protein interaction networks and the value for drug discovery. Drug Discov. Today *12*, 709–716.

79. Seath, C.P., Burton, A.J., Sun, X., Lee, G., Kleiner, R.E., MacMillan, D.W.C., and Muir, T.W. (2023). Tracking chromatin state changes using nanoscale photo-proximity labelling. Nature *616*, 574–580.

80. Nacev, B.A., Feng, L., Bagert, J.D., Lemiesz, A.E., Gao, J., Soshnev, A.A., Kundra, R., Schultz, N., Muir, T.W., and Allis, C.D. (2019). The expanding landscape of 'oncohistone' mutations in human cancers. Nature *567*, 473–478.

81. Hill, J.R., and Robertson, A.A.B. (2018). Fishing for drug targets: a focus on diazirine photoaffinity probe synthesis. J. Med. Chem. *61*, 6945–6963.

82. Shi, H., Zhang, C.-J., Chen, G.Y.J., and Yao, S.Q. (2012). Cell-based proteome profiling of potential dasatinib targets by use of affinity-based probes. J. Am. Chem. Soc. *134*, 3001–3014.

83. Ito, T., Ando, H., Suzuki, T., Ogura, T., Hotta, K., Imamura, Y., Yamaguchi, Y., and Handa, H. (2010). Identification of a primary target of thalidomide teratogenicity. science *327*, 1345–1350.

84. Gallego-Jara, J., Lozano-Terol, G., Sola-Martínez, R.A., Cánovas-Díaz, M., and de Diego Puente, T. (2020). A compressive review about Taxol®: History and future challenges. Molecules *25*, 5986.

85. Keating, G.M. (2017). Dasatinib: a review in chronic myeloid leukaemia and Ph+ acute lymphoblastic leukaemia. Drugs *77*, 85–96.

86. Montero, J.C., Seoane, S., Ocaña, A., and Pandiella, A. (2011). Inhibition of SRC family kinases and receptor tyrosine kinases by dasatinib: possible combinations in solid tumors. Clin. Cancer Res. *17*, 5546–5552.

87. Zocchi, C., Ongini, E., Conti, A., Monopoli, A., Negretti, A., Baraldi, P.G., and Dionisotti, S. (1996). The non-xanthine heterocyclic compound SCH 58261 is a new potent and selective A2a adenosine receptor antagonist. J. Pharmacol. Exp. Ther. *276*, 398–404.

88. Flaxman, H.A., Chang, C.-F., Wu, H.-Y., Nakamoto, C.H., and Woo, C.M. (2019). A binding site hotspot map of the FKBP12–rapamycin–FRB ternary complex by photoaffinity labeling and mass spectrometry-based proteomics. J. Am. Chem. Soc. *141*, 11759–11764.

89. Gao, J., Mfuh, A., Amako, Y., and Woo, C.M. (2018). Small molecule interactome mapping by photoaffinity labeling reveals binding site hotspots for the NSAIDs. J. Am. Chem. Soc. *140*, 4259–4268.

90. Huth, S.W., Oakley, J.V., Seath, C.P., Geri, J.B., Trowbridge, A.D., Parker, J.,D.L., Rodriguez-Rivera, F.P., Schwaid, A.G., Ramil, C., Ryu, K.A., et al. (2023). μMap Photoproximity Labeling Enables Small Molecule Binding Site Mapping. J. Am. Chem. Soc. *145*, 16289–16296.

91. Moss, R.A., and Doyle, M.P. (2013). Contemporary Carbene Chemistry (John Wiley & Sons).

92. Bagçi, H., Kohen, F., Kusçuoglu, U., Bayer, E.A., and Wilchek, M. (1993). Monoclonal anti-biotin antibodies simulate avidin m the recognition of biotin. FEBS Lett. *322*, 47–50.

93. Cambi, A., Joosten, B., Koopman, M., de Lange, F., Beeren, I., Torensma, R., Fransen, J.A., Garcia-Parajó, M., van Leeuwen, F.N., and Figdor, C.G. (2006). Organization of the integrin LFA-1 in nanoclusters regulates its activity. Mol. Biol. Cell *17*, 4270–4281.

94. MacGillavry, H.D., Song, Y., Raghavachari, S., and Blanpied, T.A. (2013). Nanoscale scaffolding domains within the postsynaptic density concentrate synaptic AMPA receptors. Neuron *78*, 615–622.

95. Lillemeier, B.F., Mörtelmaier, M.A., Forstner, M.B., Huppa, J.B., Groves, J.T., and Davis, M.M. (2010). TCR and Lat are expressed on separate protein islands on T cell membranes and concatenate during activation. Nat. Immunol. *11*, 90–96.

96. Murale, D.P., Hong, S.C., Haque, M.M., and Lee, J.-S. (2016). Photo-affinity labeling (PAL) in chemical proteomics: a handy tool to investigate protein-protein interactions (PPIs). Proteome Sci. *15*, 14–34.

97. Wang, H., Zhang, Y., Zeng, K., Qiang, J., Cao, Y., Li, Y., Fang, Y., Zhang, Y., and Chen, Y. (2021). Selective mitochondrial protein labeling enabled by biocompatible photocatalytic reactions inside live cells. JACS Au *1*, 1066–1075.

98. Shimada, K., Kato, H., Saito, T., Matsuyama, S., and Kinugasa, S. (2005). Precise measurement of the self-diffusion coefficient for poly (ethylene glycol) in aqueous solution using uniform oligomers. The Journal of chemical physics *122*.

99. Lemmon, M.A., and Schlessinger, J. (2010). Cell signaling by receptor tyrosine kinases. Cell *141*, 1117–1134.

100. Ogorek, A.N., Zhou, X., and Martell, J.D. (2023). Switchable DNA Catalysts for Proximity Labeling at Sites of Protein–Protein Interactions. J. Am. Chem. Soc. *145*, 16913–16923.

101. Cló, E., Snyder, J.W., Voigt, N.V., Ogilby, P.R., and Gothelf, K.V. (2006). DNA-programmed control of photosensitized singlet oxygen production. J. Am. Chem. Soc. *128*, 4200–4201.

102. Shao, Q., and Xing, B. (2012). Enzyme responsive luminescent ruthenium (II) cephalosporin probe for intracellular imaging and photoinactivation of antibiotics resistant bacteria. Chemical communications *48*, 1739–1741.

103. Ash, C., Dubec, M., Donne, K., and Bashford, T. (2017). Effect of wavelength and beam width on penetration in light-tissue interaction using computational methods. Lasers Med. Sci. *32*, 1909–1918.

104. Leyshon, L., and Reiser, A. (1972). Sensitized photodecomposition of phenyl azide and α-naphthyl azide. J. Chem. Soc., Faraday Trans. 2: Molecular and Chemical Physics *68*, 1918–1927.

105. Ikuta, K., Kina, T., MacNeil, I., Uchida, N., Peault, B., Chien, Y.-h., and Weissman, I.L. (1990). A developmental switch in thymic lymphocyte maturation potential occurs at the level of hematopoietic stem cells. Cell *62*, 863–874.

106. Kina, T., Ikuta, K., Takayama, E., Wada, K., Majumdar, A.S., Weissman, I.L., and Katsura, Y. (2000). The monoclonal antibody TER-119 recognizes a molecule associated with glycophorin A and specifically marks the late stages of murine erythroid lineage. Br. J. Haematol. *109*, 280–287.

107. Ravetz, B.D., Tay, N.E.S., Joe, C.L., Sezen-Edmonds, M., Schmidt, M.A., Tan, Y., Janey, J.M., Eastgate, M.D., and Rovis, T. (2020). Development of a platform for near-infrared photoredox catalysis. ACS Cent. Sci. *6*, 2053–2059.

108. Ásgeirsson, V., Birgisson, B.O., Bjornsson, R., Becker, U., Neese, F., Riplinger, C., and Jónsson, H. (2021). Nudged elastic band method for molecular reactions using energy-weighted springs combined with eigenvector following. J. Chem. Theory Comput. *17*, 4929–4945.

109. Nam, J.S., Kang, M.-G., Kang, J., Park, S.-Y., Lee, S.J.C., Kim, H.-T., Seo, J.K., Kwon, O.-H., Lim, M.H., Rhee, H.-W., and Kwon, T.H. (2016). Endoplasmic reticulum-localized iridium (III) complexes as efficient photodynamic therapy agents via protein modifications. J. Am. Chem. Soc. *138*, 10968–10977.